Progress In Electromagnetics Research Letters, Vol. 54, 33–38, 2015

Equivalent Verification of the Effect of the Ionospheric Faraday Rotation on GEO SAR Imaging by Ferrite

Wei-Mei Li*, Bo Liu, and Hong-Yi Zhao

Abstract—In geosynchronous earth orbit synthetic aperture radar (GEO SAR) working system, the radar signal travelling through the atmosphere is sensitive to the ionosphere. One of the effects is the Faraday rotation under geomagnetic field, which is similar to the phenomenon when the signal traveling through a ferrite medium. So based on the theoretical inference, we semi-physically simulate Faraday rotation of the ionosphere with that of the ferrite in the ground, which is one of the experiments of the ground railway prototype testing for GEO SAR system. The measurements of a mountain without ionospheric Faraday rotation and under the equivalent Faraday rotation of ionosphere are given experimentally. Imaging studies show that the influence of the ionosphere Faraday rotation on the distributed targets imaging is not visually obvious. Our work provides experimental basis for the GEO SAR to successfully image on the satellite.

1. INTRODUCTION

In recent years, a series of experimental or practical space borne SAR has found wide application in the resource monitoring, prevention of geological disasters, military reconnaissance, etc. However, present space borne SAR usually works on low-earth orbit (LEO) satellites, which are about 500–800 km above the ground. Due to its relatively small coverage on earth and long repeated observation cycle, the LEO SAR hardly satisfies the increasing need for deepening application. Working at the orbit about 36000 km above the earth, the GEO SAR has ultra-wide swath, long synthetic aperture time, short repeated observation cycle, etc. So it is meaningful for us to develop the GEO SAR for civilian and military use, and a lot of work has been done on the research of GEO SAR [1–6].

The GEO SAR system works above the ionosphere as other space borne SARs, and the wireless signal travelling through the ionosphere is affected by the ionosphere, so the SAR imaging is influenced by the ionosphere accordingly. Much work has been done [7–9] to research the effect of ionosphere on the SAR imaging. These works note that the effects of ionosphere on the pace borne SAR system are mainly phase lead, group delay, dispersion, and Faraday rotation. In the development stage of GEO SAR, it is very important to create a semi-physical simulation experiment of ionosphere on the ground before the GEO SAR working in the space. In the experiments of the ground railway prototype testing for GEO SAR system, in order to equivalent verificate the effect of the ionospheric Faraday rotation on GEO SAR imaging, this paper presents a method that semi-physically simulate Faraday rotation of the ionosphere with that of the ferrite.

2. FARADAY ROTATION IN THE IONOSPHERE

In 1845, Faraday found that some materials have optical activity in the magnetic fields parallel to the directions of light propagation, and the so-called optical activity is the polarization plane rotation that

Received 14 May 2015, Accepted 25 June 2015, Scheduled 6 July 2015
* Corresponding author: Wei-Mei Li (li_weimeihao@163.com).
The authors are with the China Academy of Space Technology (Xi'an), Xi'an, Shaanxi 710100, P. R. China.

is proportional to the strength of the magnetic fields and the traveling distance. This phenomenon is called Faraday rotation effect, and it also exists in the magnetized plasma. Ionized partly, the ionosphere is actually rarefied gas, which is mainly composed of neutral atoms and molecular, free electron and positive ions. The effect of the ionosphere in the geomagnetic field can be seen as the magnetized plasma approximately. The electromagnetic wave traveling through the ionosphere interacts with the electrons and geomagnetic field, so the polarization vector of the electric field is rotated. Following is the Faraday rotation effect from the theory.

For the plane wave traveling towards $+z$ direction in the magnetized plasma, the refractive index can be defined as: $\mathbf{n} = \mathbf{k}/k_0$, where $k_0 = \omega/c$ is the wave number in free space, and the change relations of propagating is $e^{j(\omega t - n\hat{k}z)}$, where $\hat{k}$ is the unit vector in the direction of propagation vector $\mathbf{k}$ and k the magnitude of propagation vector, so the magnitude of refractive index is $n = k/k_0$. Suppose that propagation vector $\mathbf{k}$ is parallel to magnetic fields $\mathbf{B_0}$ and $\mathbf{B_0}$ in $+z$ direction.

The angular frequency and cyclotron angular frequency of α plasma with mass of m_α and charge of $Z_\alpha e$ can be defined respectively as follows:

$$\begin{cases} \omega_{p\alpha}^2 = N_\alpha \left(Z_\alpha e\right)^2 \Big/ m_\alpha \varepsilon_0 \\ \omega_{B\alpha} = -B_0 Z_\alpha e / m_\alpha \end{cases} \tag{1}$$

The normalized frequencies of them can be presented as:

$$\begin{cases} X_\alpha = \omega_{p\alpha}^2 / \omega^2 \\ Y_\alpha = \omega_{B\alpha} / \omega \end{cases} \tag{2}$$

As for the electromagnetic wave propagates parallel to permanent magnetic field in the magnetized plasma, the dispersion relation is given by [10]:

$$\begin{cases} n_L^2 = 1 - \sum\limits_\alpha \dfrac{X_\alpha}{1 + Y_\alpha} = 1 + \sum\limits_\alpha \dfrac{\omega_{p\alpha}^2}{\omega_{B\alpha}\left(\omega_{B\alpha} + \omega\right)} \\ n_R^2 = 1 - \sum\limits_\alpha \dfrac{X_\alpha}{1 - Y_\alpha} = 1 + \sum\limits_\alpha \dfrac{\omega_{p\alpha}^2}{\omega_{B\alpha}\left(\omega_{B\alpha} - \omega\right)} \end{cases} \tag{3}$$

Of the plasma gases, electron is the lightest charged particle, and its cyclotron angular frequency is the highest. In the research of plasma made up of multi-constituents, if the electron concentration and ion concentration had the same order of magnitude, and the frequency of electromagnetic waves ω is considerably higher than cyclotron angular frequency of ion, the effect of ion can be ignored. The frequency of the ion plasma is far smaller than that of electron plasma, so only the components related to electron are retained in (3), and (3) can be expressed as:

$$\begin{cases} n_L^2 = 1 - X_e/(1 + Y_e) \\ n_R^2 = 1 - X_e/(1 - Y_e) \end{cases} \tag{4}$$

When traveling in the ionosphere at high frequency, the linear polarization wave can be decomposed into a left-hand circular polarization (LHCP) wave and a right-hand circular polarization (RHCP) wave. The two components have different refractive indeces in ionosphere, thus different speeds of spread. After traveling for a certain distance, the LHCP and RHCP waves recombine into a linear polarization wave, and the wave vector now rotates an angle compared to the incident wave vector. Following is the derivation of this angle based on the theory above.

Traveling towards $+z$ direction, for plane electromagnetic wave, its electric field has two components of $\mathbf{E_x}$ and $\mathbf{E_y}$. Now considering an x-direction linear polarization electric field at $z = 0$, it can be expressed as $\mathbf{E(t)} = \hat{x} E_0 \cos \omega t$, and it can be decomposed into two circular polarization waves as follows:

$$\mathbf{E}(t) = \mathbf{E}_L(t) + \mathbf{E}_R(t) = \left[\frac{E_0}{2}\left(\hat{x}\cos\omega t - \hat{y}\sin\omega t\right)\right] + \left[\frac{E_0}{2}\left(\hat{x}\cos\omega t + \hat{y}\sin\omega t\right)\right] \tag{5}$$

Considering the propagation factor of the electric field in $+z$ direction, the LHCP and RHCP waves can be respectively given as:

$$\begin{cases} \mathbf{E}_L\left(z,t\right) = \frac{E_0}{2}\left[\hat{x}\cos(\omega t - k_0 n_L z) - \hat{y}\sin\left(\omega t - k_0 n_L z\right)\right] \\ \mathbf{E}_R\left(z,t\right) = \frac{E_0}{2}\left[\hat{x}\cos\left(\omega t - k_0 n_R z\right) + \hat{y}\sin\left(\omega t - k_0 n_R z\right)\right] \end{cases} \tag{6}$$

Now at $z = z$, the composite electric field is:

$$\begin{aligned}\mathbf{E} &= \mathbf{E}_L(z,t) + \mathbf{E}_R(z,t) \\ &= E_0\{[\hat{x}\cos[k_0(n_R - n_L)z/2] + \hat{y}\sin(k_0(n_L - n_R)z/2)]\} \cdot \cos[\omega t - k_0(n_R + n_L)z/2]\end{aligned} \tag{7}$$

From (7), x- and y-components of the composite electric field have the same phases, so the composite wave is still a linearly polarized wave. The angle between the composite vector and the x axis is just the angle of Faraday rotation:

$$\theta = \arctan\frac{E_y}{E_x} = \arctan\frac{\sin\left[k_0(n_L - n_R)z/2\right]}{\cos\ \left[k_0\left(n_R - n_L\right)z/2\right]} = \frac{\omega}{c}\left(n_L - n_R\right)\frac{z}{2} \tag{8}$$

3. FARADAY ROTATION IN THE FERRITE

As a kind of ferromagnetic materials, the ferrite shows no anisotropy when the permanent magnet $\mathbf{H_0}$ acts by oneself, and only its permeability is strengthened. When the precession of the electron stops in the ferrite, the direction of macro spin magnetic moment $\mathbf{M_0}$ is the same as that of magnetic fields $\mathbf{H_0}$, so the ferrite is magnetized, and $\mathbf{M_0}$ is also called magnetization. If the ferrite is under the action of permanent magnet $\mathbf{H_0}$ and alternating magnetic field $\mathbf{H_1}$ together, the total magnetic field can be written as:

$$\mathbf{H} = \mathbf{H_0} + \mathbf{H_1} = \hat{x}H_{1x} + \hat{y}H_{1y} + \hat{z}(H_0 + H_{1z}) \tag{9}$$

The total magnetization $\mathbf{M}$ generated by total magnetic field $\mathbf{H}$ is:

$$\mathbf{M} = \mathbf{M_0} + \mathbf{M_1}\ = \hat{x}M_{1x} + \hat{y}M_{1y} + \hat{z}(M_0 + M_{1z}) \tag{10}$$

In Equation (10), $\mathbf{M_0} = M_0\hat{z}$ is the direct-current saturated magnetization of the ferrite under the action of permanent magnet $\mathbf{H_0}$. The saturation magnetization is one physical property of ferrite, and its typical value is $4\pi M_0 = 300\sim5000\,\mathrm{Gs}$, which can be tuned by changing H_0. For ferrite material, magnetization $\mathbf{M_1}$ is generated by alternating magnetic field $\mathbf{H_1}$, and the equations of motion for total magnetization is:

$$\frac{d\mathbf{M}}{dt} = -\gamma\left(\mathbf{M_0} + \mathbf{M_1}\right) \times \left(\mathbf{H_0} + \mathbf{H_1}\right) \tag{11}$$

For the ferrite is always working in small signal, $|\mathbf{H_1}| \ll |\mathbf{H_0}|$, and $|\mathbf{M_1}| \ll |\mathbf{M_0}|$, (11) can be simplified as follows:

$$\frac{d\mathbf{M}}{dt} = \frac{d(\mathbf{M_1} + \mathbf{M_0})}{dt} = \frac{d\mathbf{M_1}}{dt} = -\gamma\ [(\mathbf{M_0} \times \mathbf{H_1}) + (\mathbf{M_1} \times \mathbf{H_0})] \tag{12}$$

Two components can be obtained after solving (12):

$$\begin{cases} M_{1x} = \dfrac{\omega_0\omega_m H_{1x} + j\omega\omega_m H_{1y}}{\omega_0^2 - \omega^2} \\ M_{1y} = \dfrac{\omega_0\omega_m H_{1y} - j\omega\omega_m H_{1x}}{\omega_0^2 - \omega^2} \end{cases} \tag{13}$$

where precession angular frequency $\omega_0 = \gamma H_0$, intrinsic angular frequency $\omega_m = \gamma M_0$, the magnetogyric ratio γ is a constant, and its value is $1.759\times10^7\ \mathrm{rad}/(s\cdot\mathrm{Oe})$. ω is the frequency of microwave alternating field. For a RHCP magnetic field: $H_{1y}^+ = -jH_{1x}^+$ or $\mathbf{H_1^+} = H_1^+(\hat{x} - j\hat{y})$, substituting it into (13), two components can then be represented as:

$$\begin{cases} M_{1x}^+ = \dfrac{\omega_m}{\omega_0 - \omega}H_{1x}^+ = \dfrac{\omega_m}{\omega_0 - \omega}H_1^+ \\ M_{1y}^+ = \dfrac{\omega_m}{\omega_0 - \omega}H_{1y}^+ = \dfrac{-j\omega_m}{\omega_0 - \omega}H_1^+ \end{cases} \tag{14}$$

So the magnetization vector generated by $\mathbf{H_1^+}$ can be written as below:

$$\mathbf{M_1^+} = M_{1x}^+\hat{x} + M_{1y}^+\hat{y} = \frac{\omega_m}{\omega_0 - \omega}H_1^+\left(\hat{x} - j\hat{y}\right) = \frac{\omega_m}{\omega_0 - \omega}\mathbf{H_1^+} \tag{15}$$

What (15) shows is also a RHCP magnetic field, and this field rotates synchronically with excitation fields $\mathbf{H}_\mathbf{1}^+$ in angular velocity of ω. Because $\mathbf{M}_\mathbf{1}^+$ is in the same direction as $\mathbf{H}_\mathbf{1}^+$, the alternating component of total magnetic induction intensity can be expressed as:

$$\mathbf{B}_\mathbf{1}^+ = \mu_0 \left(\mathbf{H}_\mathbf{1}^+ + \mathbf{M}_\mathbf{1}^+\right) = \mu_0 \left(1 + \frac{\omega_m}{\omega_0 - \omega}\right) \mathbf{H}_\mathbf{1}^+ \tag{16}$$

So the relative permeability of RHCP wave is:

$$\mu_r^+ = \left(1 + \frac{\omega_m}{\omega_0 - \omega}\right) \tag{17}$$

The same procedure may be easily adapted to obtain relative permeability of LHCP wave:

$$\mu_r^- = \left(1 + \frac{\omega_m}{\omega_0 + \omega}\right) \tag{18}$$

So the phase constant of RHCP wave and LHCP wave are:

$$\begin{cases} \beta^+ = \omega\sqrt{\varepsilon_0\varepsilon_r\mu_0\mu_r^+} = \frac{\omega}{c}\sqrt{\varepsilon_r\mu_r^+} \\ \beta^- = \omega\sqrt{\varepsilon_0\varepsilon_r\mu_0\mu_r^-} = \frac{\omega}{c}\sqrt{\varepsilon_r\mu_r^-} \end{cases} \tag{19}$$

Now considering a linearly polarized magnetic field in x-direction at $z = 0$, which is expressed as $\mathbf{H_1}(t) = \hat{x}H_1 \cos\omega t$ and can be decomposed into two circular polarization wave:

$$\mathbf{H_1}(t) = \mathbf{H}_\mathbf{1}^+(t) + \mathbf{H}_\mathbf{1}^-(t) = \left[\frac{H_1}{2}(\hat{x}\cos\omega t + \hat{y}\sin\omega t)\right] + \left[\frac{H_1}{2}(\hat{x}\cos\omega t - \hat{y}\sin\omega t)\right] \tag{20}$$

Considering the propagation factor of the magnetic field in $+z$ direction, the RHCP and LHCP waves can be expressed separately as follows:

$$\begin{cases} \mathbf{H}_\mathbf{1}^+(z,t) = H_1\left[\hat{x}\cos\left(\omega t - \beta^+ z\right) + \hat{y}\sin\left(\omega t - \beta^+ z\right)\right] \\ \mathbf{H}_\mathbf{1}^-(z,t) = H_1\left[\hat{x}\cos\left(\omega t - \beta^- z\right) - \hat{y}\sin\left(\omega t - \beta^- z\right)\right] \end{cases} \tag{21}$$

The composite field of RHCP and LHCP fields is:

$$\mathbf{H_1}(z,t) = 2H_1\left[\hat{x}\cos\left(\frac{\beta^- - \beta^+}{2}z\right) + \hat{y}\sin\left(\frac{\beta^- - \beta^+}{2}z\right)\right] \cdot \cos\left[\omega t - \left(\frac{\beta^- + \beta^+}{2}z\right)\right] \tag{22}$$

What expressed in (22) is still a linear polarized wave. Compared to the direction of $\mathbf{H_0}$, its polarization plane rotates an angle of θ:

$$\theta = \arctan\frac{H_{1y}(z)}{H_{1x}(z)} = \arctan\frac{\sin\left(\frac{\beta^- - \beta^+}{2}z\right)}{\cos\left(\frac{\beta^- - \beta^+}{2}z\right)} = \frac{\beta^- - \beta^+}{2}z = \frac{\omega}{c}\left(\sqrt{\varepsilon_r\mu_r^+} - \sqrt{\varepsilon_r\mu_r^-}\right)\frac{z}{2} \tag{23}$$

4. EQUIVALENT VERIFICATION OF EXPERIMENT

From the above theoretical analysis of the Faraday rotation angle in ionosphere and ferrite, it can be seen that the two angles deduced from equations are symmetric in form. Except for some constant, Faraday rotation angle in ionosphere is a function of density of electrons N_e, frequency ω of electromagnetic wave, geomagnetic field B_0 and the propagation distance z, while in the ferrite, the Faraday rotation angle is a function of saturation magnetization M_0, frequency ω of electromagnetic wave, constant magnetic field H_0 and the propagation distance z. Based on the theoretical analysis above and the measurement data of ionosphere in certain place, we made a Faraday rotation simulator with ferrite to real-time simulate the Faraday rotation effects of ionosphere. Figure 1 shows a photo of Faraday rotation simulator. Figure 2 is the measured ionospheric Total Electron Conten (TEC) variation with time in a certain city of China. We measured the TEC every 15 minutes from the measuring station for one day.

Figure 1. Photograph of the Faraday rotation simulator.

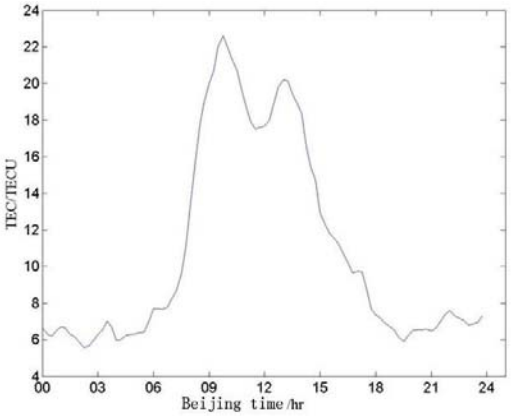

Figure 2. TEC variation curves within a day in a certain city.

Figure 3. SAR image without Faraday rotation effect.

Figure 4. SAR image under equivalent Faraday rotation effect.

Before we use these measured data of the TEC curve, these 96 data are interpolated to be one datum per second in a synthetic aperture time, and then we can get the input data of the Faraday rotation simulator from second interpolating the processed data by PRF times, here PRF is pulse repetition frequency of our radar. When we do experiments of the ground railway prototype testing for GEO SAR system in a synthetic aperture time, the Faraday rotation simulator is added in the signal transmitter and the echo receiver to simulate the round-trip Faraday rotation in the ionosphere. Figure 3 is the SAR image of surface characteristics of a mountain without Faraday rotation effect, and Figure 4 is the mountain's SAR image under the equivalent Faraday rotation effect of ionosphere. In these two figures, the directions of the mountain are contrary, because the directions in which the data were acquired are opposite. Limited for the capacity and time, we cannot provide quantitative analysis results to show the difference of the two distributed targets' SAR image; however, we can still see that the influence of the ionosphere Faraday rotation on the distributed targets imaging is not visually obvious.

5. CONCLUSION

When doing experiments of the ground railway prototype testing for GEO SAR system, a method for equivalent verification of the effect of the ionospheric Faraday rotation on GEO SAR imaging has been proposed and discussed in this paper. By employing the Faraday rotation simulator with ferrite, we can get the Faraday rotation effect of ionosphere in a limited space. Lots of theoretical analysis of Faraday rotation in ionosphere and ferrites is performed before the design of experiment. Our work provides important basic data for GEO SAR system to run successfully after the satellite is launched into space in the future.

REFERENCES

1. Tomiyasu, K., "Synthetic aperture radar in geosynchronous orbit," *IEEE Antennas and Propagation Symp.*, Vol. 16, 42–45, University of Maryland, 1978.
2. Tomiyasu, K. and J. Pacelli, "Synthetic aperture radar imaging from an inclined geosynchronous orbit," *IEEE Transactions on Geoscience and Remote Sensing*, Vol. 21, No. 3, 324–329, 1983.
3. Liu, Q., W. Hong, W. X. Tan, Y. Lin, Y. Wang, and Y. Wu, "An improved polar format algorithm with performance analysis for geosynchronous circular SAR 2D imaging," *Progress In Electromagnetics Research*, Vol. 119, 155–170, 2011.
4. Liu, Q., W. Hong, W. X. Tan, and Y. Wu, "Efficient geosynchronous circular SAR raw data simulation of extended 3-D scenes," *Progress In Electromagnetics Research*, Vol. 127, 335–350, 2012.
5. Zhao, B., X. Qi, H. Song, W. Gao, X. Han, and R. P. Chen, "The accurate fourth-order doppler parameter calculation and analysis for geosynchronous SAR," *Progress In Electromagnetics Research*, Vol. 140, 91–104, 2013.
6. Zeng, T., W. F. Yang, and Z. G. Ding, D. Liu, and T. Long, "A refined two-dimensional nonlinear chirp scaling algorithm for geosynchronous earth orbit SAR," *Progress In Electromagnetics Research*, Vol. 143, 19–46, 2013.
7. Liu, J., Y. Kuga, A. Ishimaru, et al.," Ionospheric effects on SAR imaging: A numerical study," *IEEE Transactions on Geoscience and Remote Sensing*, Vol. 41, No. 5, 939–947, 2003.
8. Anthony, F., "Calibration of linearly polarized polarimetric SAR data subject to Faraday rotation," *IEEE Transactions on Geoscience and Remote Sensing*, Vol. 42, No. 8, 1617–1624, 2004.
9. Michael, J. and R. Maurice, "Measurement of ionospheric Faraday rotation in simulated and real space borne SAR data," *IEEE Transactions on Geoscience and Remote Sensing*, Vol. 47, No. 5 1512–1523, 2009.
10. Yeh, K. C. and C. H. Liu, *Theory of Ionospheric Waves*, Academic Press, 1972.